JOC The Journal of Organic Chemistry

Article

pubs.acs.org/joc

Charge Tags for Most Comprehensive ESI-MS Monitoring of Morita–Baylis–Hillman (MBH)/*aza*-MBH Reactions: Solid Mechanistic View and the Dualistic Role of the Charge Tagged Acrylate

Renan Galaverna,*[,†] Nilton S. Camilo,[‡] Marla N. Godoi,[§] Fernando Coelho,*[,‡] and Marcos N. Eberlin[†]

[†]ThoMSon Mass Spectrometry Laboratory, Institute of Chemistry, University of Campinas - UNICAMP, P.O. Box 6154, Zip Code 13083-970, Campinas, SP, Brazil

[‡]Laboratory of Synthesis of Natural Products and Drugs, Institute of Chemistry, University of Campinas - UNICAMP, P.O. Box 6154, Zip Code 13083-970, Campinas, SP, Brazil

[§]Health Sciences Federal University of Porto Alegre - UFCSPA, Department of Pharmacoscience Sarmento Leite, Zip Code 90050-170, Porto Alegre, RS, Brazil

Supporting Information

ABSTRACT: Neutral and charge tagged reagents were used to investigate the mechanism of the classical Morita–Baylis–Hillman (MBH) reaction as well as its *aza*-version using mass spectrometry with electrospray ionization (ESI-MS). The use of an acrylate (activated alkene) with a methylimidazolium ion as a charge tag eliminates the requirement for adding acids as ESI(+) additives, which are normally used to favor protonation and therefore detection of reaction partners (reagents, intermediates, and products) by ESI(+)-MS. For both charge tagged reactions (MBH/*aza*-MBH), most reactants, intermediates, and the final adducts were efficiently detected in the form of abundant doubly and singly charged ions. Characterization of the reactions partners was performed via both tandem mass spectrometry (ESI(+)-MS/MS) and accurate *m*/*z* measurements. The charge tagged reactions also showed faster conversion rates when compare to the neutral reaction, indicating a dualistic role for the charge tagged acrylate. It acts as both the reagent and a cocatalyst due to the inherent ionic-coordination nature of the methylimidazolium ion, which stabilizes the zwitterionic intermediates and reagents through different types of coordination ion pairs. Hemiacetal intermediates for the rate-limiting proton transfer step were also intercepted and characterized for both classical and *aza*-MBH charge tagged reactions.

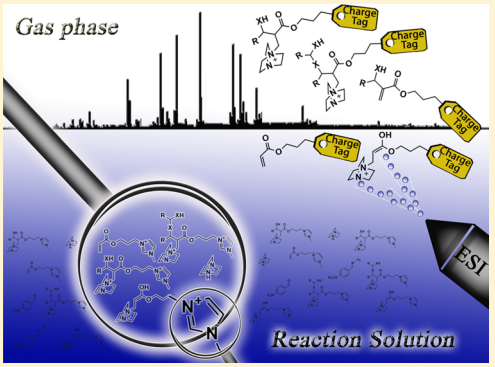

INTRODUCTION

Direct mass spectrometry (MS) monitoring of reaction solutions via spray-based techniques such as electrospray ionization (ESI-MS)[1] has become a central protocol for investigating reaction mechanisms and the actual intermediates involved.[2] ESI monitoring seems therefore to provide proper snapshots of the actual ionic composition of the reaction solution and has therefore unveiled many mechanistic details. Although there have been concerns about interferences caused by the ESI source conditions, which can be tuned to accelerate reactions rates,[3,4] no exceptional changes in such rates or the detection of unusual intermediates have been reported if conventional ESI parameters are used.[2,5] In this context, important organic reactions have been investigated by ESI-MS monitoring and some examples of these are dynamic kinetic resolution (DKR),[6] Pesci decarboxylation,[7] [2 + 2 + 2]-cycloaddition,[8] Heck and Heck-type reactions,[9] propene polymerization,[10] dephosphorylation,[11] olefin metathesis,[12] homogeneous catalysis reactions,[5] Pauson–Khand reaction,[13] Stille reaction,[14] hydro- and dehydrogenative silylation,[15] Mannich reaction,[16] and MBH/*aza*-MBH reactions.[17−20]

Such mechanistic studies have, however, been most often carried out using neutral reagents, but neutrals are undetectable by MS. Ions from such reagents and their further intermediates and products must therefore be formed in the reaction solution and later transferred to the gas phase to be detected. This requirement comes from the basic principles of ESI, which serves simply as a way to "eject" solution ions directly to the gas phase.[1] In this context, basic or acidic additives such as formic acid or ammonium hydroxide are normally used, providing a charge for the reaction partners in order to turn them into an ionic form that is suitable for ESI-MS detection.[21] The effects of such additives to the reaction outcome are, however, difficult to determine and remain unknown. In view of this concern, the use of such additives can be mostly avoided in two situations: (i) when a metal-catalyzed reaction is performed, due the charge associated to the metal when it coordinate with the reaction partners and some examples are catalysis by Au, Cu, Ag, Ir, Zr, Pd,[5,7,9,10,14] or (ii) by using a charge tag, covalently

Received: November 19, 2015
Published: December 23, 2015

DOI: 10.1021/acs.joc.5b02651
J. Org. Chem. 2016, 81, 1089−1098

Scheme 1. General Scope of MBH/*aza*-MBH Reactions

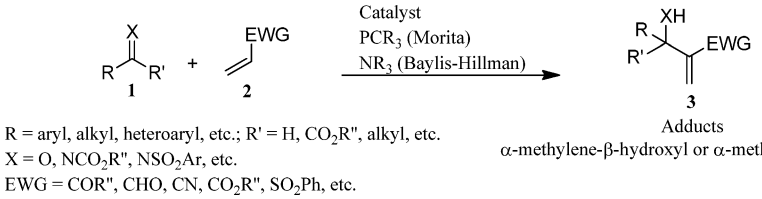

Scheme 2. MBH Mechanism Based on the McQuade and Aggarwal Proposals

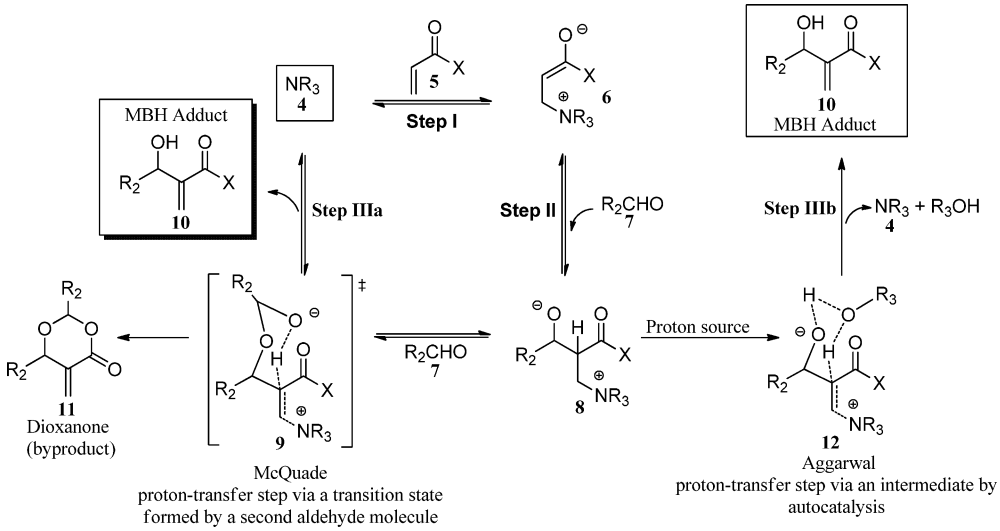

bonded to the reactants of a reaction to be monitored by ESI-MS, called a charge tagged reagent.[5,22−25] The use of charge tags seems, however, more appropriate for ESI reaction monitoring since it, in principle, guarantees that all possible intermediates involving the charge tagged reactant would have an inherent charge to facilitate the detection by MS. The charge tagging approach has, therefore, been increasingly and successfully employed in several ESI mechanistic investigations. For instance, reactions between the acetate anion bearing an imidazolium ion as the charge tag and $M(OAc)_2$ complexes (where M = Ni, Cu, and Pd; in situ reaction) to form members of a new class of charge tagged metal complexes were efficiently performed and monitored by ESI-MS.[26] Later, the catalytic performance of such palladium complexes was tested in Heck and Suzuki cross-coupling reactions, often with superior activity and yields as compared with $Pd(OAc)_2$.[26] The charge tag strategy was also used to monitor Ugi four-component condensations.[25] Hantzsch and Mannich reactions also had their mechanisms studied via charge tagged reagents.[27]

Recently, we reported comprehensive ESI-MS monitoring using charge tagged reagents to study the multicomponent Hantzsch reaction.[28] As before, the use of charge tagged reagents allowed reaction monitoring under real reaction conditions without the requirement for ESI additives. But in this study, the charge tag was placed on either, or both, of the two key reactants, that is, an aldehyde and a dicarbonyl compound. The strategy indeed facilitated the interception and characterization of most important intermediates allowing the proposal of a detailed mechanistic scheme for the Hantzsch reaction.[28]

Among the carbon−carbon bond-forming reactions, the Morita−Baylis−Hillman (MBH) and its *aza*-MBH version have been widely studied and have shown high synthetic utility.[29] The MBH reaction process with materials which are commercially available, displays high atom economy, their adducts are flexible and multifunctional, and the reaction involves a nucleophilic organocatalytic system without serious environmental impacts. The reaction conditions are also mild and can occur with high regio- and chemoselectivity.[29] MBH adducts are therefore formed when three partners are reacting: an electrophile **1** (aldehyde or imine), an activated alkene **2**, and a Lewis basic catalyst (most often tertiary amines) (Scheme 1).

Most fundamental steps of the MBH reaction have been described mainly by Morita,[30] and later by Hillman and Baylis,[31] and the initial mechanistic approach has been described by Hoffmann and Rabe[32] and Hill and Isaacs.[33] Fine MBH mechanistic details such as those operating during asymmetric induction were later proposed by Aggarwal[34] and McQuade.[35] For the mechanism therefore, the first reaction step is believed to involve a 1,4-Michael addition of the catalyst **4** (tertiary amine) to the α,β-unsaturated carbonyl compounds containing electron-withdrawing groups **5**, which generate the enolate product **6**, that is, the first zwitterionic intermediate. In step **II**, the aldol product (second zwitterionic intermediate **8**) is formed after aldolic addition of **6** to the aldehyde **7**. In the last and key proton transfer step, two mechanisms, as proposed by Aggarwal and co-workers[34] and McQuade and co-workers,[35] are still debated (Scheme 2). According to McQuade, a second aldehyde molecule is added to the aldol product in order to form the hemiacetal intermediate **9**. Now, the proton transfer involves a six-membered cyclic transition state, and the catalyst is eliminated to form the adduct **10** (step **IIIa**). This step was initially attributed as the rate-determining step (RDS) and is also able to explain the dioxanone byproduct **11** formed when X is a good leaving group.[35] However, Aggarwal showed

DOI: 10.1021/acs.joc.5b02651
J. Org. Chem. 2016, 81, 1089−1098

through supporting theoretical calculations and kinetic studies that when the MBH-adduct concentration builds up, the aldol addition step **II** becomes the RDS (Scheme 2). In this way, autocatalysis of the proton-transfer step then takes place and now protic species (adduct or solvents) by a hydrogen bond can lead to the intermediate **12**, which increases the rate conversion due to its participation in the proton transfer step (step **IIIb**). This rationale explains the autocatalytic MBH adduct effect.[34]

Most recently, Plata and Singleton re-evaluated the MBH mechanism by NMR and theoretical calculations and then proposed a new mechanism for the MBH elimination step.[36] In this new proposal, the elimination step can be thought of as a simple acid–base exchange. They proposed that the proton shuttle process as suggested by Aggarwal should be abandoned and replaced by a simple acid–base model, in which no cyclic intermediate is involved due the different bond lengths (Scheme 3).

Scheme 3. Proton Transfer Step To Form the MBH Adduct As Proposed by Plata and Singleton[36]

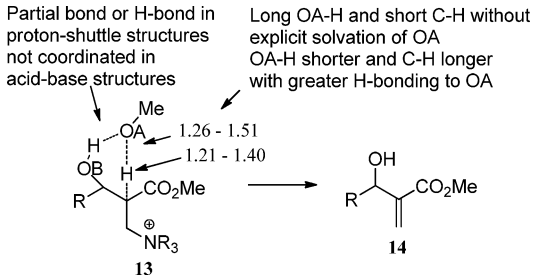

Using ESI(+)-MS monitoring, we have been systematically evaluating most mechanistic aspects of the MBH/*aza*-MBH reactions, intercepting and characterizing several of their key reaction intermediates.[17] We have also investigated the cocatalyst role of ionic liquids[18] and its dualistic nature,[19] that is, the operation of both Aggarwal and McQuade routes, and have also used a charge tagged to facilitate the detection of the intermediates.[20]

We report herein the use of the charge tag strategy to comprehensively investigate the mechanisms of the classical MBH reaction as well as its *aza*-version. Charge tags for both the aldehyde and the activated alkene were employed, and the cocatalyst action of the charge tagged reagents was also evaluated. A comparison between the neutral MBH/*aza*-MBH reactions (employing only neutral reagents) and the charge tagged reactions was also performed. Although a simplistic mechanistic view of MBH reactions has been recently proposed, based on theoretical calculations and NMR monitoring,[36] the comprehensive results herein reported using selective and highly sensitive ESI-(+)MS monitoring and the charge tag strategy allowed us to intercept intermediates that seem to be undetectable by NMR.

RESULTS AND DISCUSSION

The imidazolium ion has been shown to offer one of the most efficient charge tags to monitor reaction mechanisms by ESI(+)-MS.[37,38] In this way, we used an acrylate with a methylimidazolium ion (**5a**) and an alternate charge tag (ammonium ion) for the benzaldehyde (**7**) in the MBH ESI(+)-MS monitoring (Figure 1).

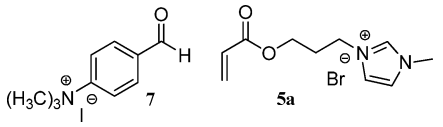

Figure 1. Charge tagged benzaldehyde and acrylate used in the MBH reaction ESI(+)-MS monitoring.

First, the classical MBH reaction was monitored using the charge tagged benzaldehyde **7** with a neutral acrylate (ethyl acrylate **5b**), 1,4-diazabicyclo[2.2.2]octane (DABCO, **4a**) as the catalyst, and acetonitrile (ACN) as the solvent. Despite many attempts to optimize the reaction as well as ESI(+)-MS conditions, the spectra (as an example see Figure S13, Supporting Information, p S9) for the classical MBH reaction were quite noisy. Furthermore, only the enolate product (first intermediate, **6**, Scheme 2) and the final MBH adduct were detected. Other intermediates, such as the aldol product (second intermediate **8**, Scheme 2) and the hemiacetal (**9**) were not detected at all. Probably, the failure to detect the aldol product was due to the high proximity of its two positive charges. This repulsive factor would be even worse for the hemiacetal due to its three positive charge centers (Scheme S1, Supporting Information, p S10). The use of the charge tagged acrylate **5a** with the neutral aldehyde (4-nitrobenzaldehyde) provided, however, very clean ESI(+) mass spectra detecting most of the expected charge tagged intermediates in high abundances. The charge tagged acrylate **5a** was therefore employed for the ESI(+)-MS monitoring of both the MBH/*aza*-MBH reactions.

For reaction monitoring therefore, the classical MBH reaction involved **5a** and 4-nitrobenzaldehyde (**7a**), DABCO (**4a**) as the catalyst, and ACN as the solvent. For the *aza*-MBH reaction, just the aldehyde **7a** was replaced by *N*-(4-methoxybenzylidene)-4-methyl-benzenesulfonamide (**7b**). For the corresponding "neutral" MBH/*aza*-MBH reactions, **5a** was replaced by ethyl acrylate (**5b**) (Scheme 4).

For monitoring, aliquots from the reaction solution were continuously taken, diluted, and then subjected to the ESI(+)-MS analysis (see Experimental Section). Figure 2 shows the ESI(+)-MS for both the neutral and charge tagged MBH/*aza*-MBH reactions at 60 min. This reaction time was selected since at 60 min the most illustrative set of intermediates were intercepted.

Note that, for both the neutral MBH/*aza*-MBH reactions (Figure 2A/B bottom), the most predominant species in the spectra after 60 min is **4a**, which is $[DABCO + H]^+$ of m/z 113. This ion predominates due to facile protonation of such a basic catalyst (pK_{aH} 8).[39] Few other intermediates such as the enolate and aldol products (**6b** of m/z 213, **8b** of m/z 364, and **8d** of m/z 502, A/B bottom) are also detected at low abundances. But unlike, the use of the charge tagged acrylate **5a** of m/z 195 offers instead a very detailed view of the reaction with the efficient interception (Figure 2A/B top) of several, if not all, key intermediates (**6a** of m/z 154, **8a** of m/z 229, **8c** of m/z 298, **9c** of m/z 443, and **9c**^{2} of m/z 587) as well as the final adducts (**10a** of m/z 346 and **10c** of m/z 484). This initial ESI(+)-MS monitoring using both neutral and charge tagged reagents proved therefore to be an efficient and sensitive strategy to obtain most intermediates of the MBH/*aza*-MBH reactions. For instance, the enolate products **6a** and **6b** (first intermediate) were unequivocally intercepted. Using theoretical calculations, NMR experiments, and kinetics estimations, Plata

DOI: 10.1021/acs.joc.5b02651
J. Org. Chem. 2016, 81, 1089–1098

Scheme 4. Mechanistic Proposal to the MBH/*aza*-MBH Reactions

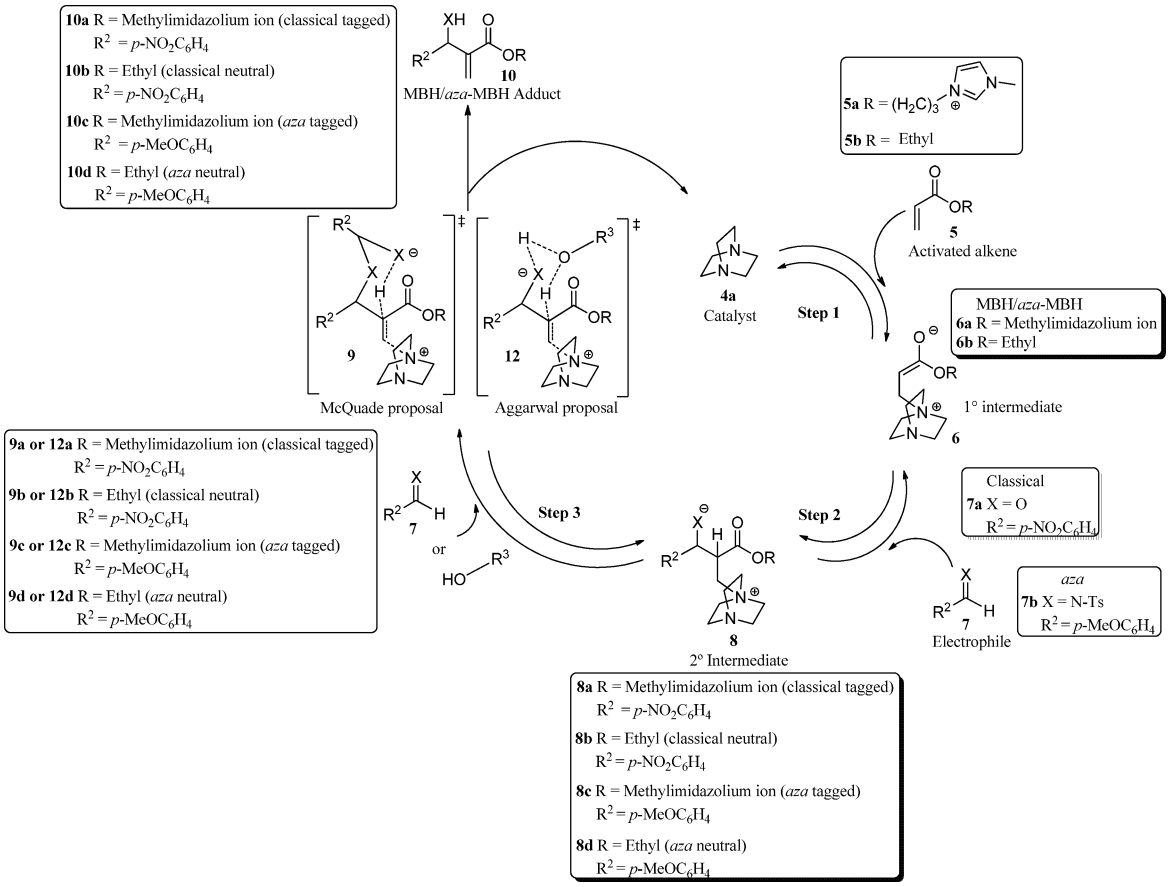

and Singleton were, however, unable to detect or theoretically find such species.[36]

Note in Figure 2A for the classical MBH reactions that the enolate and the aldol products (first and second intermediates) were intercepted in both neutral and charge tagged reactions (**6a** and **8a**, **6b** and **8b**, respectively). Note also that the final adduct **10a** could be intercepted only using the charge tagged strategy.

In Figure 2B, for the *aza*-MBH reactions, the *aza*-enolate and *aza*-aldol products (first and second intermediates) were also detected in both the charge tagged and neutral reactions, that is, **6a**/**8c** and **6b**/**8d**, respectively. For the charge tagged reaction, two additional and key doubly charge intermediates **9c** and **9c^2** were also very efficiently intercepted. ESI(+)-MS/MS and ultrahigh resolution experiments allowed us to assign **9c** and **9c^2** as hemiacetal intermediates, which are analogous to those described by McQuade[35] (Figure S17, Supporting Information, p S12). These intermediates likely have an important role in the proton transfer step due to participation of a six-membered cyclic transition state, which returns the catalyst **4a** to the catalytic cycle and leads to the final adduct (Scheme 4). The ESI(+)-MS monitoring failed to detect the autocatalytic intermediate described by Aggarwal, which also agrees with recent theoretical evaluations[20] and with the Plata and Singleton proposal.[36]

Figure 2B shows the interception of additional ions such as those of *m*/*z* 328, 402, and 601. The ion of *m*/*z* 328 was assigned to the *N*-tosyl imine potassium adduct, that is, (N-tosyl imine + K)$^+$, whereas that of *m*/*z* 402 likely results from nucleophilic attack of DABCO to the *N*-tosyl imine, that is (DABCO + N-tosyl imine + H)$^+$. ESI(+)-MS monitoring showed us that this species reverts to the starting material as the reaction proceeds. Lastly, the ion of *m*/*z* 601 was assigned as *N*-tosyl imine dimer sodium adduct [(*N*-tosyl imine)$_2$ + Na]$^+$.

Interestingly, for the charge tagged reactions, such efficient detection of the doubly charged intermediates of *m*/*z* 154 (**6a**), 229 (**8a**), 298 (**8c**), 443 (**9c**), and 587 (**9c^2**) from steps I, II, and III (Scheme 4) seems to have been facilitated during the ESI process. Considering the electrostatic models used to describe the ionization via ESI, that is, the charge residue model (CRM) and the ion evaporation model (IEM),[1] doubly charged species should indeed display higher ESI ionization and consequently MS detectabilities as compared to singly charged ions. This more efficient ion ejection would arise from doubled electrostatic repulsion occurring within ESI droplets as well as much greater preference for the doubly charged species to occupy the surface of the shrinking droplets.[40] This superior and nearly overall detectability of intermediates highlights another important aspect of the charge tag strategy for mechanistic studies that may facilitate the detection of transient intermediates which could be, for instance, undetectable by NMR.

To demonstrate the possibility of nearly continuous ESI(+)-MS monitoring, Figures 3 and 4 summarize the monitoring data by showing a temporal profile for the neutral and charge tagged MBH/*aza*-MBH reactions up to completion. Beginning with the classical MBH reactions, note that, for the neutral reaction (Figure 3A), the DABCO catalyst (**4a**) is always detected as a major ion and a significant appearance of the

DOI: 10.1021/acs.joc.5b02651
J. Org. Chem. 2016, 81, 1089−1098

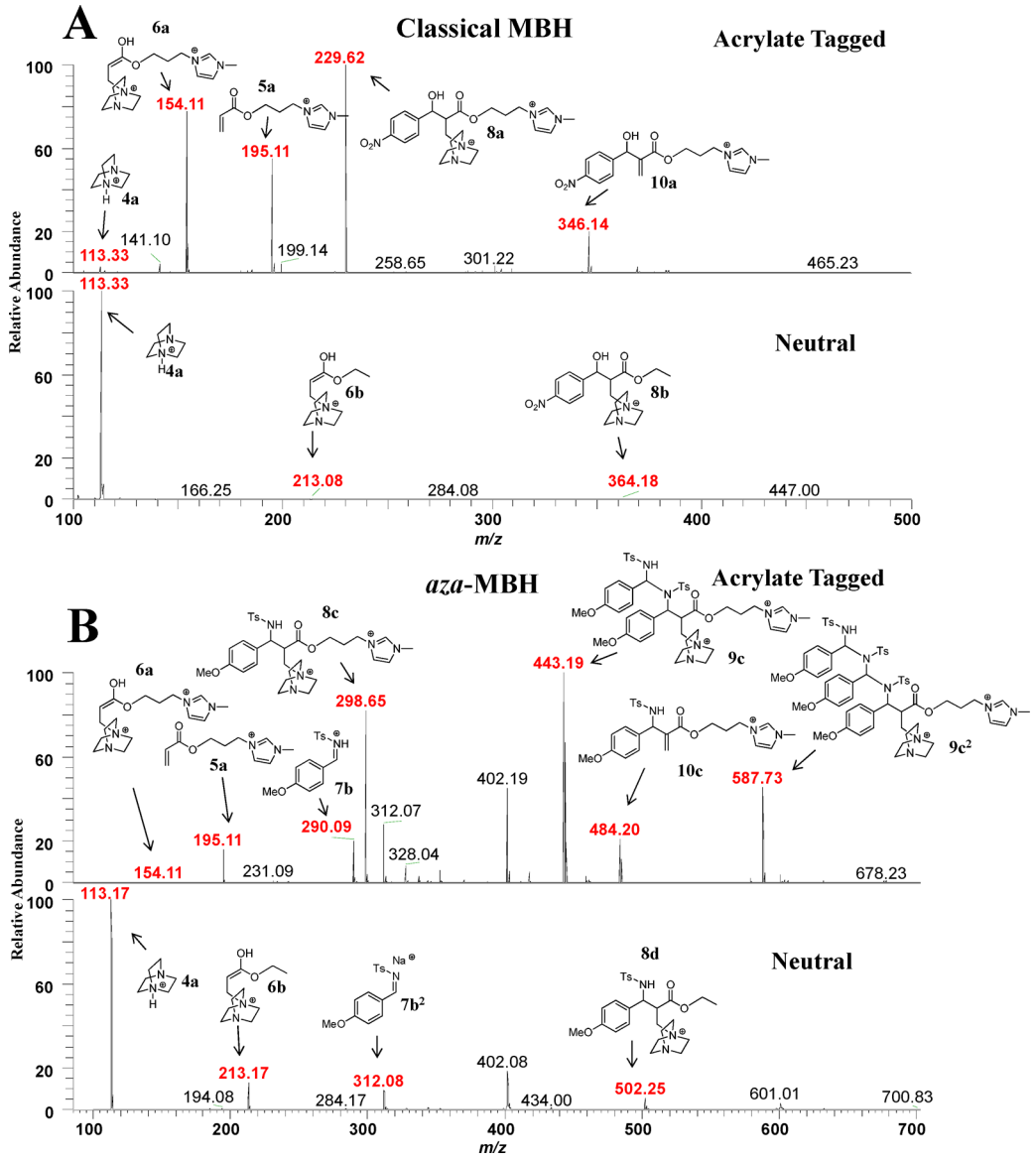

Figure 2. ESI(+)-MS of the MBH/*aza*-MBH reactions solutions at 60 min: (a) classical MBH reaction using the charge tagged acrylate **5a** (top) and ethyl acrylate **5b** (bottom); (b) *aza*-MBH reaction using **5a** (top) and **5b** (bottom).

enolate product (first intermediate **6b**) and a low abundance of the aldol product (second intermediate **8b**) can be monitored by ESI(+)-MS (10 min up to 21 h). These intermediates (**6b** and **8b**) have an expected increase and then a decrease in their abundances, leading to the adduct. At 21 h, the catalyst **4a** is again intercepted and only traces of the enolate and aldol products were detected. The final adduct was not detected at all. This failure to detect the adduct is likely due to the release of DABCO in the last step leading to an MBH adduct with no basic sites for protonation and subsequent detection (Scheme 4). Note that, in contrast, for the charge tagged reaction (Figure 3B), the reactant **5a**, the enolate and aldol products **6a** and **8a**, and the final adduct **10a** were all intercepted at high abundances. Initially (10 min), the charge tagged acrylate **5a** is the predominant ion in the spectrum (Figure 3B), but after 1 h and up to 4 h, the spectra are dominated by the enolate and aldol products (**6a** and **8a**) and the MBH adduct (**10a**). At the end of the monitoring (12 h), the MBH adduct **10a** greatly predominates. Note that the singly charged protonated DABCO catalyst **4a** is rarely detected during the whole reaction period.

Another interesting and key intermediate was detected in the beginning stage of the charge tagged reaction. This intermediate was characterized as the hemiacetal (**9a**) described by McQuade (Figure S21, Supporting Information, p S14). This initial and short time period detection corroborates with theoretical calculations reported by Aggarwal that showed that the action of such an intermediate occurs mainly up to ca. 20% adduct conversion for the classical MBH reactions.[34]

Both the neutral and charge tagged *aza*-MBH reactions were also monitored until its completion (Figure 4). The monitoring of the *aza*-MBH reactions showed similar trends to those obtained for the classical reaction. For the neutral *aza*-MBH reaction (Figure 4A), again the overall preference was for the detection of the protonated DABCO catalyst **4a**. The reactant *N*-tosyl imine in the form of a sodium adduct (**7b**^{2}) was also detected as well as the *aza*-enolate and *aza*-aldol products (**6b** and **8d**). At the beginning, 10 min, the catalyst **4a**, *N*-tosyl imine **7b**^{2}, and the *aza*-enolate and *aza*-aldol products (**6b** and

DOI: 10.1021/acs.joc.5b02651
J. Org. Chem. 2016, 81, 1089−1098

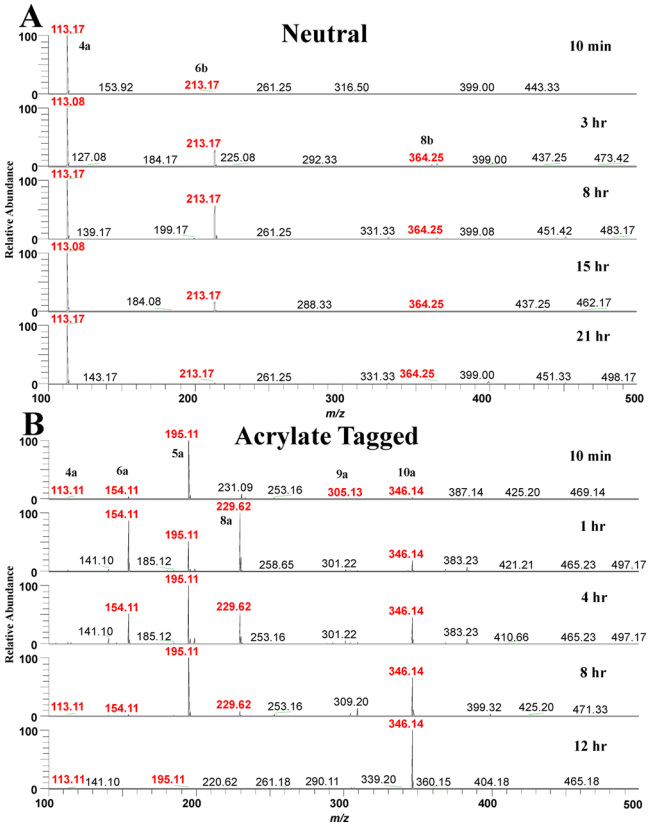

Figure 3. Temporal ESI(+)-MS monitoring for the classical MBH reaction using (a) ethyl acrylate **5b** (top) and (b) acrylate tagged **5a** (bottom).

8d) are already intercepted. From 2 h up to 20 h, there is an increase and then a decrease in their abundances, as expected, in order to form the *aza*-adduct. After 30 h, the catalyst **4a** and traces of the intermediates **6b** and **8d** and sodiated *N*-tosyl imine **7b**^{2} are detected. The *aza*-adduct with no basic sites, in the neutral reaction, was again not detected at all.

For the charge tagged reaction (Figure 4B), the formation of doubly charged intermediates such as *aza*-enolate product **8c** and the hemiacetal intermediates **9c** and **9c**^{2} as well as for the singly charged *aza*-adduct **10c** was highly beneficial for efficient ESI. Again for the intermediates, there is an expected increase and decrease in the abundances of **8c**, **9c**, and **9c**^{2}, which form the *aza*-adduct **10c**. The notable exception was for the first intermediate **6a** in the charge tagged reaction, which was detected with low abundance. Since the charge tag methylimidazolium ion should normalize all ionization efficiencies, the low abundance of the doubly charged *aza*-enolate **6a** suggests a faster conversion rate for the first intermediate of the *aza*-MBH reaction using acrylate tagged **5a**. After 22 h, the final *aza*-adduct represents the major ion with only traces of the acrylate tagged **5a**, *aza*-aldol product **8c**, and the hemiacetal **9c** and **9c**^{2} (Figure 4B).

A most notable feature therefore for the ESI(+)-MS monitoring of the charge tagged MBH/*aza*-MBH reactions was the interception of the doubly charged hemiacetal intermediates. Their proper characterization via accurate mass measurements and ESI(+)-MS/MS experiments could therefore be performed. For the neutral reaction, such intermediates remained undetectable even when using a molar excess of either *N*-tosyl imine or 4-nitrobenzaldehyde.

The data from Figures 3B and 4B are also summarized via the plots of Figure 5, which allows us to follow the relative changes in abundance for the charge tagged reactions including reagents, intermediates, and final adducts as a function of reaction time. Note the much higher conversion rate for the classical MBH since even at t = 0 the final adduct is already detected as one of the most abundant ions whereas for the *aza*-MBH it becomes a major ion only after 10 h. For the classical reaction a nearly constant contribution is seen for the catalyst ion, i.e., protonated DABCO (**4a**). There is a decrease for **4a** during the course of the reaction but a return to the original abundance as the reaction comes to its end. For the hemiacetal intermediates, a major difference is noted between the *aza* and classical MBH reactions. For the *aza*-MBH reaction, both hemiacetal intermediates (**9c** and **9c**^{2}) are detected as quite abundant ions during the whole reaction period with a normal up and down pattern. On the other hand, the short detection time of the hemiacetal for the classical MBH charge tagged reaction was not enough to set via plot in Figure 5.

Another key feature for the charge tagged reactions was the conversion rate. The total reaction time for the charge tagged reactions (Figures 3 and 4) was substantially lower than that for the corresponding neutral reactions. For the classical MBH reaction, a more dramatic (ca. 50%) decrease was observed, from 21 to 12 h. For the *aza*-MBH reaction, a decrease of ca. 30% was observed, that is, from 30 to 22 h. We have showed that imidazolium ionic liquids (IL) act as a cocatalyst for the MBH reactions, and supramolecular species formed by coordination of neutral reagents, adducts, and the protonated forms of zwitterionic intermediates with cations and anions of ionic liquids have been characterized by ESI(+)-MS.[18] The interception of these supramolecular species indicated the IL cocatalyst's role, which acts in the mechanism to activate both electrophiles (aldehyde and activated alkene) toward nucleophilic attack and/or to stabilize the zwitterionic intermediates that constitute the main MBH intermediates. Based on these findings, the cocatalyst action of the methylimidazolium ion for the acrylate **5a** could be rationalized as contributing in the mechanism steps as shown in Scheme S2 in Supporting Information, p S10.

To demonstrate this intrinsic high conversion rate due to the cocatalyst effect of the charge tagged **5a**, we monitored the charge tagged reactions by HPLC-ESI-MS as well as the neutral reaction by TLC until their completion. Table 1 summarizes the results and confirms the dual role of the charge tagged acrylate **5a**.

■ CONCLUSIONS

The use of a charge tagged acrylate **5a** allowed comprehensive ESI(+)-MS monitoring of both MBH/*aza*-MBH reactions. Most reagents, intermediates, and MBH adducts could be efficiently and directly transferred by ESI from the reaction solutions to the gas phase for proper ultrahigh resolution and tandem MS characterization. Superior detectability was promoted by the formation of doubly charged species. The hemiacetal interception for both MBH/*aza*-MBH agrees with our previous reports indicating the formation of this intermediate.[19] The dual cocatalyst role of the charge tagged acrylate **5a** was also demonstrated. A detailed temporal monitoring of the reactions was also possible which allowed for the observation of the rising and fading of all reaction partners for the successive reaction steps.

DOI: 10.1021/acs.joc.5b02651
J. Org. Chem. 2016, 81, 1089−1098

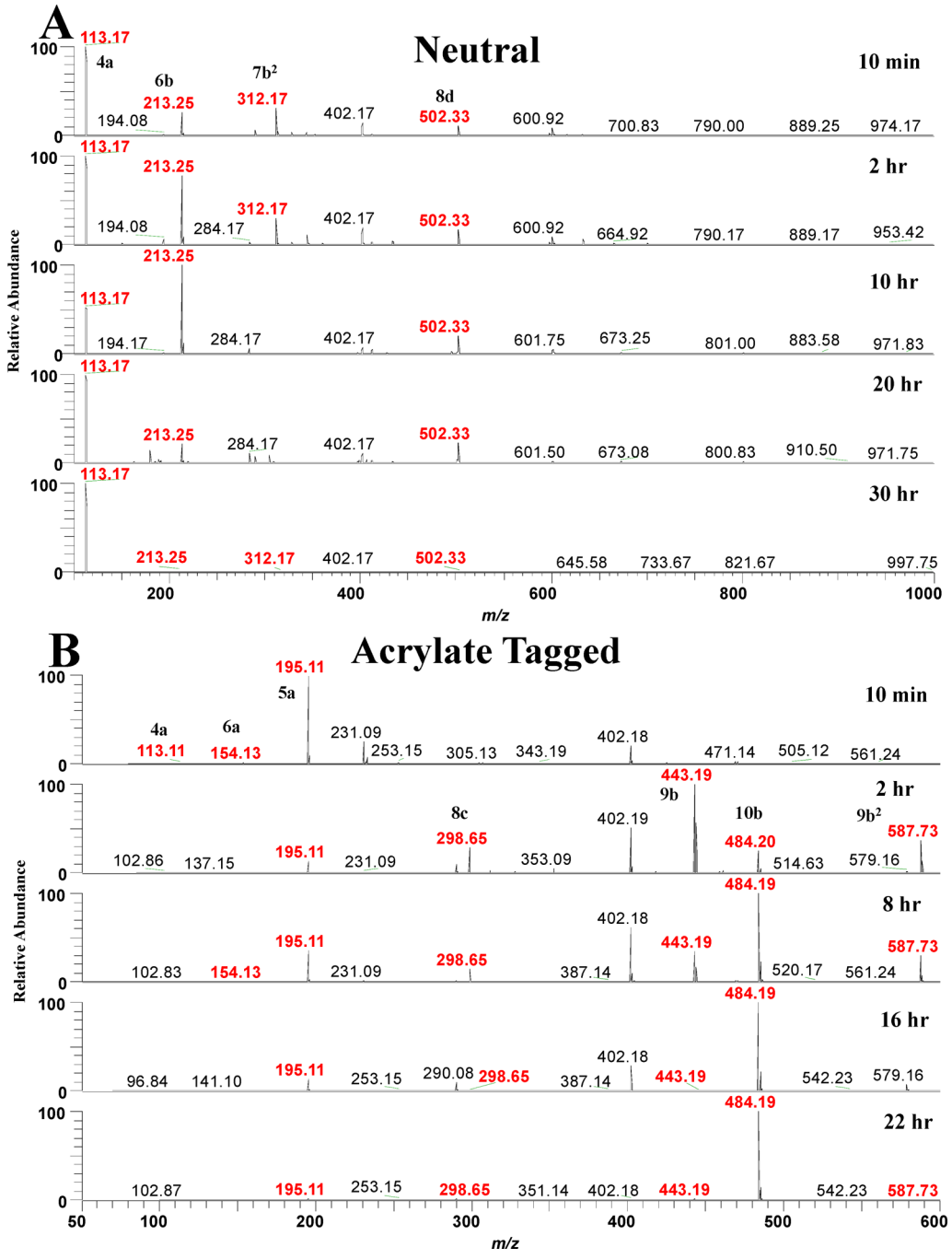

Figure 4. Temporal ESI(+)-MS monitoring of *aza*-MBH reaction using (a) ethyl acrylate **5b** (top) and (b) acrylate tagged **5a** (bottom).

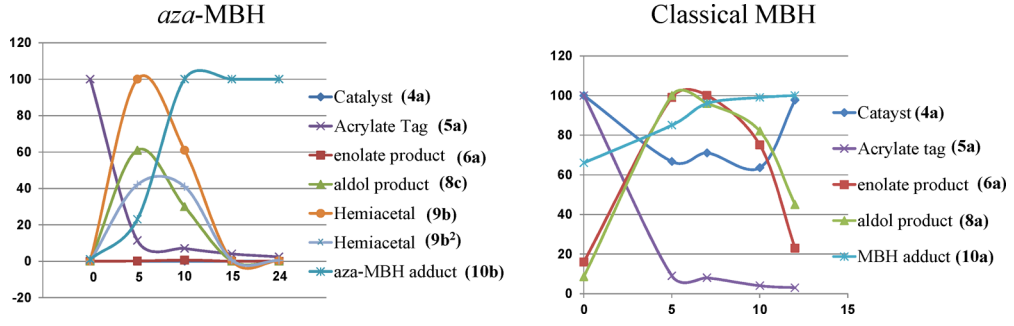

Figure 5. Temporal monitoring for both the charge tagged MBH/*aza*-MBH reactions.

DOI: 10.1021/acs.joc.5b02651
J. Org. Chem. 2016, 81, 1089−1098

Table 1. Cocatalyst Role of the Charge Tagged Acrylate 5a for the MBH/*aza*-MBH Reactions

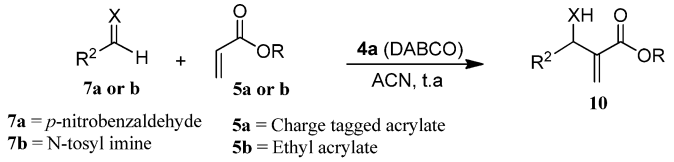

7a = *p*-nitrobenzaldehyde
7b = N-tosyl imine
5a = Charge tagged acrylate
5b = Ethyl acrylate

Charge tagged MBH/*aza*-MBH reactions (R = $(H_2C)_3$ imidazolium)					Neutral MBH/*aza*-MBH reactions (R = Ethyl)				
Entry	Aldehyde /Imine	R^2	Time (h)	Yield (%)	Entry	Aldehyde /Imine	R^2	Time (h)	Yield (%)
1 (**10a**)	X = O	*p*-$NO_2C_6H_4$	12[a]	60	2 (**10b**)	X = O	*p*-$NO_2C_6H_4$	21[b]	90
3 (**10c**)	X = N-Ts	*p*-$MeOC_6H_4$	22[a]	55	4 (**10d**)	X = N-Ts	*p*-$MeOC_6H_4$	30[b]	74

[a]Determined by HPLC-ESI-MS. [b]Determined by TLC.

EXPERIMENTAL SECTION

General Methods. All reactions were carried out under air, in a round-bottom flask with magnetic stirring, unless otherwise noted. Commercially available reagents and solvents were used without further purification. ^{1}H and ^{13}C NMR spectra were recorded on a 250 MHz instrument. Chemical shifts (δ) are given in parts per million. The following abbreviations were used to designate chemical shift multiplicities: s = singlet, d = doublet, dd = doublet of doublets, t = triplet, q = quartet, quint. = quintuplet, m = multiplet. High-resolution mass spectra data were recorded on a 7.2T LTQ-FT Ultra mass spectrometer.

Procedure for Preparing 1-[3-(Acryloyloxy)propyl]-3-methylimidazolium Bromide (5a). In a sealed tube of 100 mL containing a magnetic stirrer were added 1-methylimidazole (328 mg, 4 mmol), 3-bromo-1-propanol (690 mg, 5 mmol), and dry acetonitrile (10 mL). The reaction mixture was refluxed at 90 °C for 24 h and monitored by thin layer chromatography (TLC). After cooling at room temperature, solvent was removed and the residue was dissolved in water (2 mL) and extracted with ethyl acetate (5 × 5 mL). The organic layers were combined and dried over Na_2SO_4, and the solvent was removed under reduced pressure. Afterward, the residue was kept under a high vacuum line for 3 h. Colorless viscous liquid, 98% yield (884 mg, 3.9 mmol). **Spectroscopic data:** 1-(3-Hydroxypropyl)-3-methylimidazolium bromide, **^{1}H NMR** (250 MHz, CD_3OD) δ 2.05 (quint, J = 6.7 Hz, 2H); 3.56 (t, J = 6 Hz, 2H); 3.91 (s, 3H); 3.92 (s, 1H); 4.31 (t, J = 6 Hz, 2H); 7.55 (s, 1H) 7.62 (s, 1H) 8.94 ppm (s, 1H). **^{13}C NMR** (62.5 MHz, D_2O) δ 31.7; 35.8; 46.6; 58.0; 122.4; 123.7; 136.2 ppm. **HRMS** (ESI, m/z): calculated for $C_7H_{13}N_2O^+$ 141.1022; found 141.1024.

Subsequently, in order to prepare the tagged acrylate (**5a**), in a round-bottom flask of 25 mL, 1-(3-hydroxypropyl)-3-methyl-imidazolium bromide (alcohol tagged) (141 mg, 1 mmol) was mixed with acryloyl chloride (108 mg, 1.2 mmol). The reaction mixture was kept at room temperature for 4 h. After its completion, the reaction medium was concentrated under reduced pressure and the residue was dissolved in water (2 mL) and extracted with ethyl acetate (5 × 5 mL). The organic layers were combined and dried over Na_2SO_4, and the solvent was removed under reduced pressure. Afterward, the residue was kept under a high vacuum line for 3 h. Colorless viscous liquid, 98% yield (0.269 mg, 0.98 mmol). **Spectroscopic data:** 1-Methyl-3-[3-(prop-2-enoyloxy)propyl]-1*H*-imidazol-3-ium bromide (**5a**), **^{1}H NMR** (250 MHz, CD_3OD) δ 1.88 (quint, J = 6.7 Hz, 2H); 3.94 (s, 3H); 4.24 (t, J = 6 Hz, 2H); 4.37 (t, J = 6 Hz, 2H); 5.93−5.88 (dd, J = 1.6 and 10.3 Hz, 1H); 6.17−6.10 (dd, J = 10.3 and 17.2 Hz, 1H); 6.41−6.34 (dd, J = 1.6 and 17.2 Hz, 1H) 7.60 (s, 1H) 7.69 (s, 1H) 9.03 ppm (s, 1H). **^{13}C NMR** (62.5 MHz, CD_3OD) δ 28.9; 35.3; 46.7; 60.9; 122.4; 123.7; 127.8; 130.7; 136.8; 166.0 ppm. **HRMS** (ESI, m/z): calculated for $C_{10}H_{15}N_2O_2^+$ 195.1128; found 195.1127.

Experimental Data for Compounds of Table 1. *3-[3-({2-[Hydroxy(4-nitrophenyl)methyl]prop-2-enoyl}oxy)propyl]-1-methyl-1H-imidazol-3-ium Bromide (**10a**, entry 1).* In a round-bottom flask of 10 mL containing a magnetic stirrer were mixed acrylate **5a** (0.21 g, 0.5 mmol, 1 equiv), 4-nitrobenzaldehyde (0.151 g, 1 mmol, 2 equiv), and DABCO (0.034 g, 0.6 mmol, 0.6 equiv) in acetonitrile (500 μL). The reaction evolution was monitored with a UPLC−MS instrument using a Hypersil Gold C18 column, and the mobile phase employed was a mixture of water/acetonitrile 50:50 v/v. After completion (12 h), solvent was removed and the residue was dissolved in water (2 mL) and extracted with ethyl acetate (5 × 5 mL). The organic layers were combined and dried over Na_2SO_4, and the solvent was removed under reduced pressure. Afterward, the residue was kept under a high vacuum for 3 h to afford the corresponding MBH adduct **10a** as a yellow viscous liquid, 60% yield (255 mg, 0.6 mmol). **^{1}H NMR** (250 MHz, CD_3OD) δ 2.21 (quint., J = 6.6 Hz, 2H); 3.92 (s, 3H); 4.17 (t, J = 6.0 Hz, 2H); 4.24 (t, J = 7.0 Hz, 2H); 5.68 (s, 1H); 6.08 (s, 1H); 6.37 (s, 1H); 7.61 (m, 4H); 8.19 (d, 2H). **^{13}C NMR** (62.5 MHz, CD_3OD) δ 28.7; 31.3; 35.1; 61.0; 62.4; 70.8; 122.3; 123.0; 123.6; 125.4; 127.7; 142.5; 147.3; 149.9; 166.9. **HRMS** (ESI, m/z): calculated for $C_{17}H_{20}N_3O_5^+$ 346.1397; found 346.1404.

*Ethyl 2-[Hydroxy(4-nitrophenyl)methyl]prop-2-enoate (**10b**, entry 2).* In a round-bottom flask of 10 mL containing a magnetic stirrer were mixed ethyl acrylate (54 μL, 0.5 mmol, 1 equiv), 4-nitrobenzaldehyde (0.151 g, 1 mmol, 2 equiv), and DABCO (0.034 g, 0.6 mmol, 0.6 equiv) in acetonitrile (500 μL). The reaction was stirred for 21 h at room temperature, and its evolution was monitored by thin layer chromatography (TLC). After completion, the solvent was removed and the residue was purified by flash column chromatography (SiO_2, gradient: Hex; 9/1 Hex/AcOEt; 8/2 Hex/AcOEt) to give MBH adduct **10b** as a pale yellow oil (113 mg, 0.45 mmol, 90%). **^{1}H NMR** (250 MHz, CD_3OD) δ 1.25 (t, J = 7.1 Hz, 3H); 3.42 (s, 1H); 4.14 (q, J = 7.1 Hz, 2H); 5.61 (s, 1H); 5.85 (s, 1H); 6.38 (s, 1H); 7.56 (d, J = 8.7 Hz, 2H); 8.18 (d, J = 8.6 Hz, 2H). **^{13}C NMR** (62.5 MHz, CD_3OD), δ 14.0; 61.3; 72.7; 123.5; 127.0; 127.3; 141.2; 147.4; 148.7; 166.0. **HRMS** (ESI, m/z) calculated for $C_{12}H_{13}NNaO_5^+$ 274.0686; found: 274.0679.

*3-[3-({2-({[(4-Methanesulfonylphenyl)methyl]amino}(4-methoxyphenyl)methyl)prop-2-enoyl}oxy)propyl]-1-methyl-1H-imidazol-3-ium Bromide (**10c**, entry 3).* In a round-bottom flask of 10 mL containing a magnetic stirrer were mixed acrylate **5a** (0.137 g, 0.5 mmol, 1 equiv), *N*-(4-methoxybenzylidene)-4-methyl-benzenesulfonamide (0.289 g, 1 mmol, 2 equiv), and DABCO (0.034 g, 0.6 mmol, 0.6 equiv) in acetonitrile (500 μL). The reaction was monitored with a UPLC−MS instrument using a Hypersil Gold C18 column, and the mobile phase employed was a mixture of water/acetonitrile 50:50 v/v. After completion (22 h), solvent was removed and the residue

DOI: 10.1021/acs.joc.5b02651
J. Org. Chem. 2016, 81, 1089−1098

obtained was dissolved in water (2 mL). Then, the aqueous phase was extracted with ethyl acetate (5 × 5 mL). The organic layers were combined and dried over Na_2SO_4, and the solvent was removed under reduced pressure. Afterward, the residue was kept under high vacuum for 3 h to furnish *aza*-MBH adduct **10c**, as an orange viscous oil in 55% yield (158 mg, 0.28 mmol). **^{1}H NMR** (250 MHz, CD_3OD) δ 2.34 (quint, J = 6.5 Hz, 3H); 2.52 (s, 3H); 3.85 (s, 3H); 4.06 (s, 3H); 4.32 (m, J = 7.1 Hz, 4H); 5.49 (s, 1H); 5.91 (s, 1H); 6.40 (s, 1H); 6.85 (d, J = 8.8 Hz, 2H); 7.06 (d, J = 8.6 Hz, 2H); 7.37 (d, J = 8.0 Hz, 2H); 7.71 (m, J = 7.8 Hz, 4H); 9.03 (s, 1H). **^{13}C NMR** (62.5 MHz, CD_3OD), δ 20.0; 28.7; 35.2; 54.4; 57.0; 61.1; 113.4; 122.2; 123.6; 126.1; 126.7; 128.4; 128.9; 129.0; 129.5; 130.3; 138.1; 140.9; 143.1; 159.2; 165.6. **HRMS** (ESI, m/z) calculated for $C_{25}H_{30}N_3O_5S^+$ 484.1901; found: 484.1893.

*Ethyl 2-[(4-Methoxyphenyl)(4-methylbenzenesulfonamido)-methyl]prop-2-enoate (**10d**, entry 4).* In a round-bottom flask of 10 mL containing a magnetic stirrer were mixed ethyl acrylate (54 μL, 0.5 mmol, 1 equiv), *N*-(4-methoxybenzylidene)-4-methyl-benzenesulfonamide (0.289 g, 1 mmol, 2 equiv), and DABCO (0.034 g, 0.6 mmol, 0.6 equiv) in acetonitrile (500 μL). The reaction was stirred for 30 h at room temperature, and its evolution was followed by thin layer chromatography (TLC). After completion, the solvent was removed under reduced pressure and the residue was purified on silica gel by flash column chromatography (SiO_2, gradient: Hex; 9/1 Hex/AcOEt; 8/2 Hex/AcOEt) to furnish the *aza*-MBH adduct **10d**, as a pale yellow viscous oil, in 74% yield (144 mg, 0.37 mmol). **^{1}H NMR** (250 MHz, CD_3OD) δ 1.15 (t, J = 7.1 Hz, 3H); 2.4 (s, 3H); 3.74 (s, 3H); 4.05 (q, J = 7.1 Hz, 2H); 5.25 (d, J = 8.5 Hz, 1H); 5.60 (d, J = 8.6 Hz, 1H); 5.8 (s, 1H); 6.20 (s, 1H); 6.74 (d, J = 8.8 Hz, 2H); 7.04 (d, J = 8.0 Hz, 2H); 7.22 (d, J = 8.0 Hz, 2H); 7.66 (d, J = 8.3 Hz, 2H). **^{13}C NMR** (62.5 MHz, CD_3OD) δ 13.9; 21.47; 55.2; 58.5; 60.9; 113.8; 127.2; 127.7; 129.4; 130.8; 137.6; 138.9; 143.3; 159.1; 165.4. **HRMS** (ESI, m/z) calculated for $C_{20}H_{23}NNaO_5S^+$ 412.1189; found: 412.1191.

General Procedure for Reactions Monitoring. All reactions monitored by ESI(+)-MS were prepared in a round-bottom flask of 10 mL with a magnetic stirrer containing 0.6 equiv of catalyst (DABCO), 1 equiv of alkene activated (acrylate tagged or ethyl acrylate), 2 equiv of electrophile (aldehyde or *N*-tosyl imine), and 500 μL of acetonitrile as the reaction solvent at ambient temperature. Aliquots from the reaction medium (1 μL) were continuously taken and diluted in 1 mL of acetonitrile (ACN). The sample solutions were prepared in polypropylene microtubes (Eppendorf) and directly injected into the ESI(+)-FT-ICR-MS.

Mass Spectrometry Data. For this exploratory mechanistic study, ultrahigh resolution MS data were performed using a 7.2T LTQ-FT Ultra mass spectrometer equipped with a direct infusion electrospray ionization source operating in the positive mode ESI(+)-MS under the following conditions: Spray Voltage, 3.5 kV; Capillary Potential, 40 V; Tube lens potential, 100 V; Capillary Temperature, 280 °C, and a Flow rate of 10 μL/min. Data were recorded in full MS mode in ESI(+) using a range of m/z 100 to 1000. The average resolving power (Rp) was 200.000 at m/z 400, where Rp was calculated as $M/\Delta M_{50\%}$, that is, the m/z value divided by the peak width at 50% peak height. Mass spectra were the result of over 10 microscans and processed via the Xcalibur software.

The ESI(+)-MS/MS experiments were performed on the same mass spectrometer operating as a Linear Ion Trap (LTQ). The isolation width (0−2) and collision energy (0−30) were adjusted for each experiment in order to achieve the best results. ESI(+)-MS/MS data were processed via the Xcalibur software.

■ ASSOCIATED CONTENT

Supporting Information

The Supporting Information is available free of charge on the ACS Publications website at DOI: 10.1021/acs.joc.5b02651.

ESI(+)-MS/MS and mass measurements data for the MBH/*aza*-MBH reactions; NMR spectra (PDF)

■ AUTHOR INFORMATION

Corresponding Authors

*E-mail: renan.galaverna@iqm.unicamp.br.

*E-mail: coelho@iqm.unicamp.br.

Notes

The authors declare no competing financial interest.

■ ACKNOWLEDGMENTS

The authors are grateful to Fundação de Amparo à Pesquisa do Estado de São Paulo (Fapesp) for research fund (Nos. 2013/10449-5 and 2012/10701-3) and CNPq for research fellowships (F.C. and M.N.E.).

■ REFERENCES

(1) Banerjee, S.; Mazumdar, S. *Int. J. Anal. Chem.* **2012**, *2012*, 1−40 (Article ID 282574).10.1155/2012/282574

(2) (a) Schroder, D. *Acc. Chem. Res.* **2012**, *45*, 1521−1532. (b) O'Hair, R. A. J. *Int. J. Mass Spectrom.* **2015**, *377*, 121−129. (c) Chen, P. *Angew. Chem., Int. Ed.* **2003**, *42*, 2832−2847.

(3) Girod, M.; Moyano, E.; Campbell, D. I.; Cooks, R. G. *Chem. Sci.* **2011**, *2*, 501−510.

(4) Lee, J. K.; Banerjee, S.; Nam, H. G.; Zare, R. N. *Q. Rev. Biophys.* **2015**, *48*, 437−444.

(5) Vikse, K. L.; Ahmadi, Z.; McIndoe, J. S. *Coord. Chem. Rev.* **2014**, *279*, 96−114.

(6) Vaz, B. V.; Milagre, C. D. F.; Eberlin, M. N.; Milagre, H. M. S. *Org. Biomol. Chem.* **2013**, *11*, 6695−6698.

(7) O'Hair, R. A. J.; Rijs, N. J. *Acc. Chem. Res.* **2015**, *48*, 329−340.

(8) Parera, M.; Dachs, A.; Solà, M.; Pla-Quintana, A.; Roglans, A. *Chem. - Eur. J.* **2012**, *18*, 13097−13107.

(9) (a) Sabino, A. A.; Machado, A. H. L.; Correia, C. R. D.; Eberlin, M. N. *Angew. Chem., Int. Ed.* **2004**, *43*, 2514−2518. (b) Enquist, P. A.; Nilsson, P.; Sjoberg, P.; Larhed, M. *J. Org. Chem.* **2006**, *71*, 8779−8786. (c) Fernandes, T. A.; Vaz, B. V.; Eberlin, M. N.; da Silva, A. J. M.; Costa, P. R. R. *J. Org. Chem.* **2010**, *75*, 7085−7091. (d) Skillinghaug, B.; Sköld, C.; Rydfjord, J.; Svensson, F.; Behrends, M.; Savmarker, J.; Sjöberg, P. J. R.; Larhed, M. *J. Org. Chem.* **2014**, *79*, 12018−12032.

(10) Vatamanu, M. *J. Catal.* **2015**, *323*, 112−120.

(11) Silva, M.; Mello, R. S.; Farrukh, M. A.; Venturini, J.; Bunton, C. A.; Milagre, H. M. S.; Eberlin, M. N.; Fiedler, H. D.; Nome, F. *J. Org. Chem.* **2009**, *74*, 8254−8260.

(12) Adlhart, C.; Hinderling, C.; Baumann, H.; Chen, P. *J. Am. Chem. Soc.* **2000**, *122*, 8204−8214.

(13) Henderson, M. A.; Luo, J. W.; Oliver, A.; McIndoe, J. S. *Organometallics* **2011**, *30*, 5471−5479.

(14) Santos, L. S.; Rosso, G. B.; Pilli, R. A.; Eberlin, M. N. *J. Org. Chem.* **2007**, *72*, 5809−5812.

(15) Vicent, C.; Viciano, M.; Mas-Marza, E.; Sanau, M.; Peris, E. *Organometallics* **2006**, *25*, 3713−3720.

(16) Milagre, C. D. F.; Milagre, H. M. S.; Santos, L. S.; Lopes, M. L. A.; Moran, P. J. S.; Eberlin, M. N.; Rodrigues, J. A. R. *J. Mass Spectrom.* **2007**, *42*, 1287−1293.

(17) Santos, L. S.; Pavam, C. H.; Almeida, W. P.; Coelho, F.; Eberlin, M. N. *Angew. Chem., Int. Ed.* **2004**, *43*, 4330−4333.

(18) Santos, L. S.; Neto, B. A. D.; Consorti, C. S.; Pavam, C. H.; Almeida, W. P.; Coelho, F.; Dupont, J.; Eberlin, M. N. *J. Phys. Org. Chem.* **2006**, *19*, 731−736.

(19) Amarante, G. W.; Milagre, H. M. S.; Vaz, B. G.; Ferreira, B. R. V.; Eberlin, M. N.; Coelho, F. *J. Org. Chem.* **2009**, *74*, 3031−3037.

(20) Rodrigues, T. S.; Silva, V. H. C.; Lalli, P. M.; de Oliveira, H. C. B.; da Silva, W. A.; Coelho, F.; Eberlin, M. N.; Neto, B. A. D. *J. Org. Chem.* **2014**, *79*, 5239−5248.

(21) Eberlin, M. N. *Eur. Mass Spectrom.* **2007**, *13*, 19−28.

(22) Santos, V. G.; Godoi, M. N.; Regiani, T.; Gama, F. H.; Coelho, M. B.; de Souza, R. O.; Eberlin, M. N.; Garden, S. J. *Chem. - Eur. J.* **2014**, *20*, 12808−12816.

DOI: 10.1021/acs.joc.5b02651
J. Org. Chem. 2016, 81, 1089−1098

(23) Lalli, P. M.; Rodrigues, T. S.; Arouca, A. M.; Eberlin, M. N.; Neto, B. A. D. *RSC Adv.* **2012**, *2*, 3201−3203.
(24) Souza, R. Y.; Bataglion, G. A.; Ferreira, D. A. C.; Gatto, C. C.; Eberlin, M. N.; Neto, B. A. D. *RSC Adv.* **2015**, *5*, 76337−76341.
(25) Medeiros, G. A.; da Silva, W. A.; Bataglion, G. A.; Ferreira, D. A. C.; de Oliveira, H. C. B.; Eberlin, M. N.; Neto, B. A. D. *Chem. Commun.* **2014**, *50*, 338−340.
(26) Oliveira, F. F. D.; dos Santos, M. R.; Lalli, P. M.; Schmidt, E. M.; Bakuzis, P.; Lapis, A. A. M.; Monteiro, A. L.; Eberlin, M. N.; Neto, B. A. D. *J. Org. Chem.* **2011**, *76*, 10140−10147.
(27) Alvim, H. G. O.; Bataglion, G. A.; Ramos, L. M.; de Oliveira, A. L.; de Oliveira, H. C. B.; Eberlin, M. N.; de Macedo, J. L.; da Silva, W. A.; Neto, B. A. D. *Tetrahedron* **2014**, *70*, 3306−3313.
(28) Santos, V. G.; Godoi, M. N.; Regiani, T.; Gama, F. H.; Coelho, M. B.; de Souza, R. O.; Eberlin, M. N.; Garden, S. J. *Chem. - Eur. J.* **2014**, *20*, 12808−12816.
(29) For some reviews concerning the MBH reaction, see: (a) Shi, M.; Wang, F.-J.; Zhao, M.-X.; Wei, Y. *The Chemistry of the Morita−Baylis−Hillman Reaction*; RSC Publishing: Cambrigde, U.K., 2011. (b) Basavaiah, D.; Veeraraghavaiah, D. G. *Chem. Soc. Rev.* **2012**, *41*, 68 and references cited therein.
(30) Morita, K.; Suzuki, Z.; Hirose, H. *Bull. Chem. Soc. Jpn.* **1968**, *41*, 2815−2815.
(31) Hillman, M. E.; Baylis, A. B. U.S. Patent 3,743,669, Jul 3, 1973.
(32) Hoffmann, H. M. R.; Rabe, J. *Angew. Chem., Int. Ed. Engl.* **1983**, *22*, 795−796.
(33) Hill, J. S.; Isaacs, N. S. *J. Phys. Org. Chem.* **1990**, *3*, 285−288.
(34) (a) Aggarwal, V. K.; Fulford, S. Y.; Lloyd-Jones, G. C. *Angew. Chem., Int. Ed.* **2005**, *44*, 1706−1708. (b) Robiette, R.; Aggarwal, V. K.; Harvey, J. N. *J. Am. Chem. Soc.* **2007**, *129*, 15513−15525.
(35) (a) Price, K. E.; Broadwater, S. J.; Walker, B. J.; McQuade, D. T. *J. Org. Chem.* **2005**, *70*, 3980−3987. (b) Price, K. E.; Broadwater, S. J.; Jung, H. M.; McQuade, D. T. *Org. Lett.* **2005**, *7*, 147−150.
(36) Plata, R. E.; Singleton, D. A. *J. Am. Chem. Soc.* **2015**, *137*, 3811−3826.
(37) Dupont, J.; Eberlin, M. N. *Curr. Org. Chem.* **2013**, *17*, 257−272.
(38) Limberger, J.; Leal, B. C.; Monteiro, A. L.; Dupont, J. *Chem. Sci.* **2015**, *6*, 77−94.
(39) Benoit, R. L.; Lefebvre, D.; Fréchette, M. *Can. J. Chem.* **1987**, *65*, 996−1001.
(40) Tang, K.; Smith, R. D. *J. Am. Soc. Mass Spectrom.* **2001**, *12*, 343−347.

DOI: 10.1021/acs.joc.5b02651
J. Org. Chem. 2016, 81, 1089−1098